Interface states at SiO_2/6*H*-SiC(0001) interfaces observed by x-ray photoelectron spectroscopy measurements under bias: Comparison between dry and wet oxidation

Hikaru Kobayashi,* Takeaki Sakurai,† and Masao Takahashi
Institute of Scientific and Industrial Research, Osaka University, Osaka 567-0047, Japan
and CREST, Japan Science and Technology Corporation, 8-1, Mihogaoka, Ibaraki, Osaka 567-0047, Japan

Yasushiro Nishioka
Tsukuba Research and Development Center, Japan Texas Instruments, Miyukigaoka, Tsukuba, Ibaraki 305-0841, Japan
(Received 31 July 2002; published 5 March 2003)

Interface states in almost the entire SiC band gap are observable by means of x-ray photoelectron spectroscopy (XPS) measurements under bias, although SiC is a wide-gap semiconductor having 2.9 eV band-gap energy. When a SiO_2 layer is formed by wet oxidation at 1000 °C on 6*H*-SiC(0001) Si-faced surfaces, only a broad interface state peak is observed at ~2 eV above the SiC valence-band maximum (VBM), while for dry oxidation at the same temperature, an additional sharp interface state peak is caused at 1.8 eV above the VBM. When the wet-oxidation temperature is increased to 1150 °C, this 1.8-eV interface-state peak also appears. The concentration of graphitic carbon at the SiO_2/SiC interface is found to increase with the heat treatment temperature. The 1.8-eV interface-state peak is tentatively attributed to graphitic carbon with a special structure near the interface. On the other hand, the broad 2-eV interface-state peak is attributed to Si dangling bonds at the interface. Without the 1.8-eV interface-state peak, current-voltage (*I*-*V*) curves measured under x-ray irradiation deviate only slightly from the ideal *I*-*V* curve (~0.4 V), while with this peak, the deviation becomes much larger (~0.8 V). XPS measurements under bias show that the *I*-*V* curves under x-ray irradiation are determined by the magnitude of band bending in SiC. Therefore, the deviation from the ideal *I*-*V* curve is attributed to the accumulation of holes (i.e., minority carriers), generated by x-ray irradiation, at interface states with energies between the SiC and metal Fermi levels, causing a downward SiC band-edge shift and thus resulting in a decrease in the magnitude of band bending in SiC. This result demonstrates that the interface states affect *I*-*V* characteristics by a static effect (i.e., interface state charges), not by a dynamical effect (i.e., electron-hole recombination at the interface states).

DOI: 10.1103/PhysRevB.67.115305 PACS number(s): 73.20.At, 79.60.Jv, 73.40.Qv

I. INTRODUCTION

SiC is a wide-gap semiconductor (band gap of 6*H*-SiC: 2.9 eV) (Ref. 1) which is chemically and thermally more stable than Si, and thus its application to devices under severe conditions is expected. In fact, SiC-based devices can work at high temperatures ranging 300–650 °C.[2] Moreover, SiC possesses excellent physical properties such as a high thermal conductivity of 4.9 $W\,cm^{-1}\,K^{-1}$, a high breakdown electrical field of 4 $MV\,cm^{-1}$, a high electron drift velocity of 2.0×10^7 cm/s, etc.[3] From these properties, SiC is desirable for application to power devices[4] and high-frequency devices.[5] In the case of applications to metal-oxide-semiconductor (MOS) technology, another advantage lies in the fact that SiO_2 layers can be formed by the direct thermal oxidation of SiC. However, the thermal oxidation of SiC requires high temperatures above 1050 °C, i.e., higher by ~200 °C than Si oxidation. High-temperature oxidation causes degradation in interfacial properties such as an increase in the interface-state density,[6–9] and thus good electrical characteristics expected from the excellent physical properties are not achieved. Therefore, the observation of interface-state spectra is of importance for the improvement of the MOS characteristics. For the formation of SiO_2 layers on SiC, wet oxidation in water-containing oxygen atmospheres is believed to generate lower interface-state density than dry oxidation.[10,11] It is also reported that the interface-state density is strongly dependent on the oxidation temperatures.[7,10] In the case of clean SiC(0001) surfaces with a (3×3) reconstruction produced in an ultrahigh-vacuum system, oxidation proceeds at lower temperatures (500–650 °C) with no formation of carbon species.[12,13]

For the observation of interface states in the SiC band gap, electrical techniques such as capacitance-voltage[6,8–10,14–16] (*C*-*V*) and conductance-voltage[6–8,15,16] (*G*-*V*) measurements are usually employed. Using the electrical technique, however, interface states only in the limited energy region are observable because deep interface states possess too large time constants to respond to the ac signal. The energy of the deepest interface states, E_{dp}, with respect to the *n*-type SiC conduction-band minimum (CBM) is given by[17]

$$E_{dp}=kT\ln\frac{eN_{it}\sigma_n\nu_{\rm th}K(T)}{C_{\rm ox}R}, \tag{1}$$

where N_{it} is the total interface state density in cm^{-2}, σ_n is the electron capture cross section, $\nu_{\rm th}$ is the electron thermal velocity, $C_{\rm ox}$ is the capacitance of an oxide layer, R is the ramp rate in $V\,s^{-1}$, and $K(T)$ is equal to $3.97\times10^{16}\ T^{1.5}\,cm^{-3}$. Inserting reported values [e.g., $10^{13}\ cm^{-2}$ for N_{it}, $10^{-17}\ cm^2$ for σ_n, $10^7\ cm\,s^{-1}$ for $\nu_{\rm th}$, $2\times10^{-7}\ F\,cm^{-2}$ for $C_{\rm ox}$, and $0.002\ V\,s^{-1}$ for R (Refs. 8 and

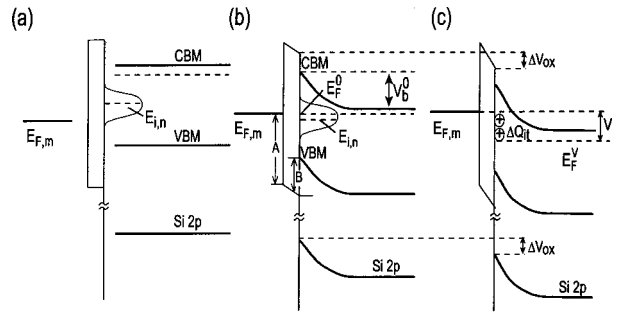

FIG. 1. Band diagrams of *n*-type SiC-based MOS diodes (a) before contact, (b) after contact at zero bias, and (c) after contact under a positive bias applied to SiC with respect to metal.

18)], E_{dp} at 298 K is estimated to be 0.83 eV. This estimation shows that interface states present only near the majority-carrier band (i.e., conduction band for *n*-SiC) are observable by means of *C*-*V* and *G*-*V* techniques. Interface states too close to the majority-carrier band [closer than 0.2 eV (Ref. 15)], on the other hand, respond to both high and low frequencies, also leading to the underestimation of the interface state density.

Under UV light irradiation during *C*-*V* measurements (i.e., photo-*C*-*V* technique), deep interface states respond to electrical signals, but only the total interface-state density can be obtained using this technique.[19,20]

In the present study, the energy distribution of interface states in almost the entire SiC band-gap region is obtained using the spectroscopic and static techniques recently developed by us [i.e., x-ray photoelectron spectroscopy (XPS) measurements under bias[21–25]]. Under x-ray irradiation, electron-hole pairs are generated and interface states equilibrate with the valence or conduction bands due to the presence of these charges.[25] The measurements clearly show that the interface-state spectra are greatly affected by the oxidation type (i.e., dry or wet oxidation) and the oxidation temperature. Interface states are found to affect the current-voltage (*I*-*V*) characteristics by changing the band bending in SiC.

II. THEORETICAL PRINCIPLE

Four kinds of charges (i.e., interface state charges Q_{it}, depletion layer charges Q_D, oxide-fixed charges $Q_{\rm fix}$, and their countercharges at the metal/SiO_2 interface, Q_m) are assumed to be present in the interfacial region of SiC-based MOS structure. From the charge neutrality, we have

$$Q_m = -(Q_{it} + Q_D + Q_{\rm fix}). \tag{2}$$

Figures 1(a) and 1(b) show band diagrams before and after contact, respectively. The interface neutral level $E_{i,n}$ before contact is assumed to be located between the metal Fermi level and SiC Fermi level. After contact, all the Fermi levels coincide due to electron transfer from the SiC substrate to the interface states and that from the interface states to the metal. Due to the charge transfer, the interface states between $E_{i,n}$ and the interface Fermi level E_F^0 are newly occupied by electrons. Therefore, using Eq. (2), we have

$$e\int_{E_F^0}^{E_{i,n}} D_{it}(E)dE + (2eN_D\varepsilon_s V_b^0)^{1/2} + eN_{\rm fix} = (1/e)(E_F^0 - E_{F,m})C_{\rm ox}, \tag{3}$$

where E_F^0 and $E_{i,n}$ are defined with respect to the SiC valence-band maximum (VBM), D_{it} is the interface state density as a function of the energy, *E*, in the SiC band gap, N_D is the donor density, ε_S is the permittivity of SiC, V_b^0 is the SiC band bending at zero bias, $N_{\rm fix}$ is the density of oxide fixed charges, $E_{F,m}$ is the metal Fermi level before contact with respect to the SiC VBM, and $C_{\rm ox}$ is the capacitance of the SiO_2 layer. In Eq. (3), the abrupt junction approximation is employed for the estimation of Q_D.

At zero bias [Fig. 1(b)] interface states present below E_F^0 are occupied by electrons, while those above E_F^0 are empty. By the application of a positive bias *V* to SiC, the SiC Fermi level E_F^V deviates downward from the metal Fermi level $E_{F,m}$ by the magnitude of *V* [Fig. 1(c)]. Consequently, the interface states present between $E_{F,m}$ and E_F^V become unoccupied (i.e., accumulation of positive charges at the interface states). Under x-ray irradiation, electron-hole pairs are generated in SiC, and holes are transferred to the SiO_2/SiC interface by the electrical field in the space-charge layer. Therefore, interface states equilibrate with the SiC valence band even if they are deep states. A change in the charge concentration, ΔQ_V, induced by the bias *V* is given by

$$\Delta Q_V = e\int_{E_F^V}^{E_F^0} D_{it}(E)dE + (2eN_D\varepsilon_S)[(V_b^V)^{1/2} - (V_b^0)^{1/2}], \tag{4}$$

where V_b^V is the SiC band bending under bias *V* which is written as

$$V_b^V = V_b^0 + V - \Delta Q_V/C_{\rm ox}. \tag{5}$$

These bias-induced charges cause a change in the potential drop across the oxide layer, $\Delta V_{\rm ox}$, with the magnitude given by

$$\Delta V_{\rm ox} = \Delta Q_V/C_{\rm ox} = \left[e\int_{E_F^V}^{E_F^0} D_{it}(E)dE + (2eN_D\varepsilon_s)^{1/2} \times \{(V_b^V)^{1/2} - (V_b^0)^{1/2}\} \right] \Big/ C_{\rm ox}. \tag{6}$$

Since the energy difference between the metal Fermi level and SiO_2 band at the metal/SiO_2 interface [denoted by *A* in Fig. 1(b)] that between the SiO_2 and Si bands at the SiO_2/SiC interface (denoted by *B*) and that between the SiC band and the SiC core levels (e.g., Si 2*p* level) are constant, the SiC core level at the interface is shifted by $\Delta V_{\rm ox}$, and this shift is observable by means of XPS. It should be noted that the depletion layer width estimated from the donor density is $\sim$0.5 μm, much longer than the mean free path of photoelectrons (2–3 nm).[26] Therefore, the photoelectron signal due to the substrate core level arises only from the interfacial region in which the SiC band can be regarded as flat. It is also noted that a change in the depletion layer charges [second term in

Eq. (6)] causes ΔV_{ox} with a magnitude of only 40 mV at maximum: negligibly small compared to ΔV_{ox} induced by interface-state charges. (The maximum ΔV_{ox} observed in the present study is ~1 V.) Therefore, we have

$$\Delta V_{ox} \approx e \int_{E_F^V}^{E_F^0} D_{it}(E) dE / C_{ox}. \quad (7)$$

On the other hand, E_F^V is given by

$$E_F^V = E_F^0 - eV + e\,\Delta V_{ox}. \quad (8)$$

Therefore, using Eqs. (7) and (8), the energy distribution of interface states (i.e., D_{it} as a function of energy E in the band gap) can be obtained from measurements of ΔV_{ox} (i.e., bias-induced shift of the substrate SiC core level) at various bias voltages V.

The interfacial Fermi level E_F^0 is determined from measurements of the energy difference between the Pt 4*f* and Pt Fermi levels of the thick Pt film (E_1), that between the substrate Si 2*p* level and the SiC valence-band maximum of the SiC surface (E_2), and that between the Si 2*p* and Pt 4*f* levels of the ⟨Pt/SiO_2/6*H*-SiC(0001)⟩ structure (E_3) using the following equation (E_1, E_2, and E_3 are defined to have positive values):

$$E_F^0 = E_1 + E_2 - E_3. \quad (9)$$

III. EXPERIMENTS

6*H*-SiC(0001) Si-face wafers having a nitrogen-doped *n*-type epitaxial layer of 10 μm thickness with a donor density of 6×10^{15} cm^{-3} were cleaned using the RCA method. Silicon dioxide (SiO_2) layers were formed by heat treatments at 1000 or 1150 °C in wet or dry oxygen. (Hereafter, these oxide layers are called wet oxide and dry oxide, respectively.) In some cases, post-oxidation annealing (POA) was performed at 950 or 1150 °C in nitrogen for 20 h. Then 3-nm-thick platinum (Pt) layers were deposited by an electron beam evaporation method, resulting in the ⟨Pt/SiO_2/6*H*-SiC(0001)⟩ MOS structure. Ohmic contact at the rear SiC surface was achieved by the deposition of a nickel film followed by heat treatment at 900 °C.

X-ray photoelectron spectroscopy spectra were measured using a VG Scientific Escalab 220*i*-XL spectrometer with a monochromatic Al $K\alpha$ radiation source. X rays were irradiated from the Pt layer side, and photoelectrons were collected in the surface-normal direction. The electron pass energy in the hemispherical analyzer was set at 10 eV. During the XPS measurements, the front Pt layer was grounded and a bias voltage was applied to the rear Si surface. The energy of the Pt 4*f* peak of the overlayer measured at each bias voltage was taken as the energy reference.

The current-voltage (I-V) curves for ⟨Pt/SiO_2/6*H*-SiC(0001)⟩ MOS diodes were recorded without and with Al $K\alpha$ x-ray irradiation, using an HP 4140B PA meter-voltage source.

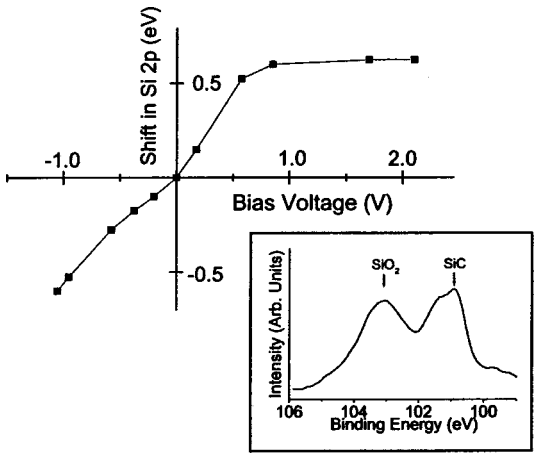

FIG. 2. Plot of the shift of the substrate Si 2*p* peak for the ⟨Pt/SiO_2/6*H*-SiC(0001) Si face⟩ MOS structure with the SiO_2 layer formed at 1000 °C in dry oxygen vs the bias voltage applied to SiC with respect to Pt. The inset shows the XPS spectra in the Si 2*p* region measured at zero bias.

IV. RESULTS

The inset of Fig. 2 shows the XPS spectrum in the Si 2*p* region measured at zero bias for the ⟨Pt/SiO_2/6*H*-SiC(0001)⟩ MOS structure with the ultrathin SiO_2 layer formed at 1000 °C in dry oxygen. An asymmetrical peak was due to the overlapping of the Si $2p_{3/2}$ and $2p_{1/2}$ levels of the SiC substrate and a broad peak to the SiO_2 layer. From the ratio in the area intensity of the SiO_2 peak to that of the substrate peak, the SiO_2 thickness was estimated to be 3.1 nm.

Figure 2 plots the shift of the substrate Si 2*p* peak versus the bias voltage for the ⟨Pt/SiO_2/6*H*-SiC(0001)⟩ MOS diodes with the SiO_2 layer formed at 1000 °C in dry oxygen. By the application of a negative bias to the SiC substrate with respect to the Pt overlayer, the substrate peak was shifted toward lower binding energy, while upon application of a positive bias, the peak shifted in the higher-energy direction. The broad oxide peak also shifted in the same direction, but its magnitude was much smaller.[27] These shifts were completely reversible (i.e., by the removal of the bias voltage, the shift always disappeared) in contrast to chemical shifts which are irreversible, and thus these shifts could be attributed to bias-induced charges in interface states. In the positive-bias region, which corresponded to the energy below the interfacial Fermi level, the shift increased with the bias voltage up to ~1 V. Beyond 1 V the shift almost stopped, indicating that the interface-state density was negligibly low in this voltage region. This shift also increased with the negative-bias voltage up to ~−1 V, and a further increase of the negative-bias voltage simply resulted in an increase in the IR drop in the Pt layer due to a high-density leakage current, but the interfacial Fermi level did not rise anymore.

Figure 3 shows the energy distribution of the interface-state density obtained from the analysis of the energy shift of the substrate Si 2*p* peak versus the bias voltage (e.g., Fig. 2). It should be noted that interface states in the whole SiC

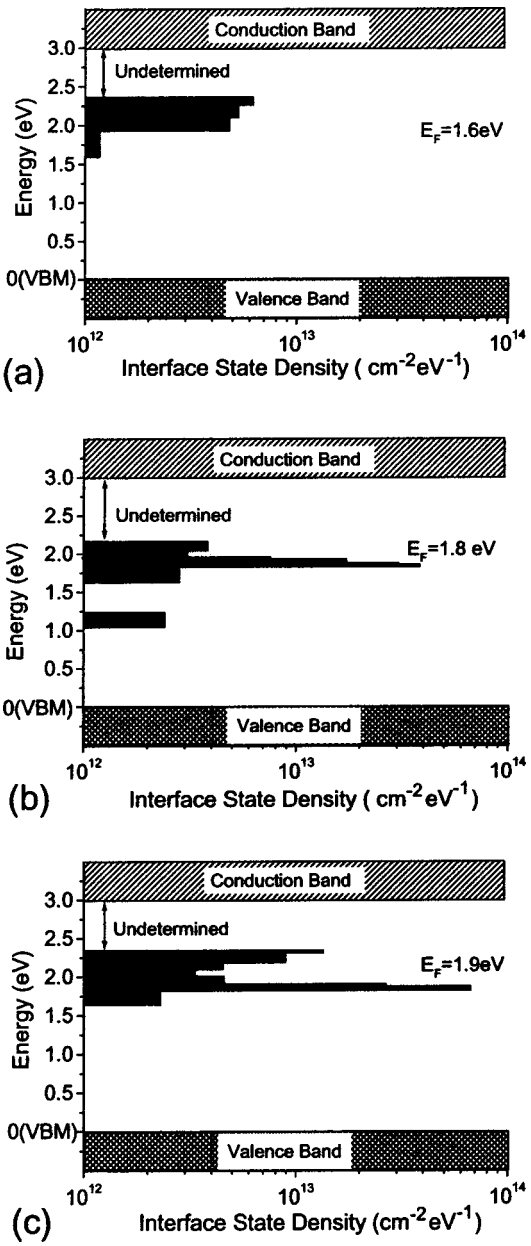

FIG. 3. Interface-state spectra obtained from XPS measurements under bias for the $\langle Pt/SiO_2/6H\text{-}SiC(0001)$ Si face$\rangle$ MOS structure with the SiO_2 layer formed under the following conditions: (a) at 1000 °C in wet oxygen, (b) at 1150 °C in wet oxygen, and (c) at 1150 °C in dry oxygen.

band-gap region are observable by means of XPS measurements under bias as long as the interfacial Fermi level can be shifted by the bias. This is because holes generated by x rays (or electrons) are transferred to the SiC/SiO_2 interface and they equilibrate with interface states.[25] (The undetermined regions in the spectra correspond to the bias regimes where an increase in the bias voltage is consumed by the IR drop in the Pt layer due to the high current density.)

For the SiO_2 layers formed by thermal oxidation at 1000 °C in wet oxygen, only a broad interface state peak centered at ~2 eV was present in the interface-state spectrum (spectrum *a*). When the oxidation temperature was increased to 1150 °C, a sharp peak was observed at 1.8 eV in addition to the broad structure (spectrum *b*). For thermal oxidation in dry oxygen at 1000 °C, the 1.8-eV sharp peak was observed with a higher intensity and the broad structure was also present (spectrum *c*). For all the SiC-based MOS diodes investigated, the density of interface states was considerably low below 1.5 eV with respect to the VBM.

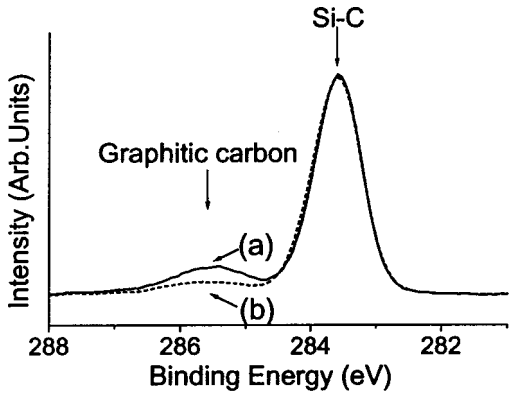

FIG. 4. XPS spectra in the C 1*s* region for the ~2-nm $SiO_2/SiC(0001)$ Si face structure measured after the following POA treatments: (a) at 950 °C in nitrogen and (b) at 1150 °C in nitrogen.

Figure 4 shows the XPS spectra in the C 1*s* region. In this case, 75-nm-thick SiO_2 layers were initially formed followed by POA in nitrogen at 950 or 1150 °C for 20 h. Then the SiO_2 layers were etched with 1% hydrofluoric acid. The etching was stopped when both the substrate and oxide Si 2*p* peaks were observed with considerable intensities at the same time (SiO_2 thickness: ~2 nm). At this etching point, two peaks were observed in the C 1*s* XPS spectrum for the SiO_2 layers with POA at 1150 °C (spectrum *a*), and the lower- and higher-energy peaks were attributable to SiC and graphitic carbon, respectively.[28,29] For the SiO_2 layers with POA at 950 °C (spectrum *b*), the intensity of the peak due to graphitic carbon became much lower (spectrum *b*). The takeoff angle-dependent measurements showed that graphitic carbon for spectrum *b* was present mainly on the SiO_2 surface, and thus it was attributable to contamination, the concentration of which was estimated to be 0.4–0.5 monolayer. For thick SiO_2 layers, we also observed a weak peak due to graphitic carbon attributable to contamination, and its concentration was also found to be 0.4–0.5 monolayer. For spectrum *a*, on the other hand, graphitic carbon was found from the takeoff angle-dependent measurements to be present mainly near the SiO_2/SiC interface. After subtracting the intensity due to contamination from spectrum *a*, the concentration of graphitic carbon at the interface was estimated to be 2 monolayers, assuming that the rest of graphitic carbon was present at the SiO_2/SiC interface.

The concentration of interfacial graphitic carbon without POA was low even when the SiO_2 layer had been formed at 1150 °C in dry oxygen and the C 1*s* spectrum was nearly the same as spectrum *b* in Fig. 4. This is probably because, although graphitic carbon was formed at such a high temperature, most of it reacted with oxygen, resulting in the formation of CO and thus in desorption. In the case of the SiO_2

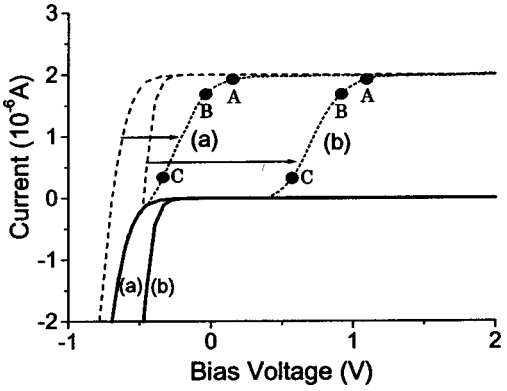

FIG. 5. I-V curves for the $\langle Pt/SiO_2/6H$-SiC(0001) Si face$\rangle$ MOS structure with the SiO_2 layer formed under the following conditions: (a) at 1000 °C in wet oxygen and (b) at 1000 °C in dry oxygen. The solid and dotted lines show the I-V curves measured without and with x-ray irradiation, respectively. The dashed lines show the ideal I-V curves under x-ray irradiation. Points $A-C$ denote the bias voltages at which the magnitudes of the SiC band bending are identical.

layer with POA at high temperatures in nitrogen, on the other hand, the produced graphitic carbon accumulates at the interface because of the absence of oxidizing species. It should be noted that graphitic carbon in 0.4–0.5 monolayer due to contamination was always present at the surface and the detection limit of the interfacial graphitic carbon was ~0.5 monolayer. It is highly probable that when the oxidation temperature is high, interfacial graphitic carbon with a concentration less than 0.5 monolayer is present even without POA.

Figure 5 shows the I-V curves for the $\langle Pt/SiO_2/6H$-SiC(0001)$\rangle$ MOS diodes measured without (solid lines) and with x-ray irradiation (dotted lines). Due to the ultrathin SiO_2 layers, tunneling currents flowed and the diodes showed rectifying characteristics. The I-V curve without irradiation for the wet-oxide layers formed at 1000 °C was observed in a more negative-bias region by ~0.2 V than that for the dry-oxide layers at the same temperature. This voltage difference agrees with the difference in the interfacial Fermi level: i.e., 1.6 eV above the VBM for the wet-oxide layers and 1.8 eV for the dry-oxide layers (cf. Fig. 3).

The ideal I-V curve under x-ray irradiation is simply given by the parallel shift of the dark I-V curve by the magnitude of the photocurrent density,[30] as depicted by the dashed lines. The observed I-V curve under x-ray irradiation for the 1000 °C wet-oxide layer deviated by ~0.4 V from the ideal I-V curve, while that for the dry-oxide layer deviated by ~0.8 V.

V. DISCUSSION

X-rays generate electron-hole pairs in SiC, and in the presence of the upward band bending in SiC, generated holes transfer to the SiC/SiO_2 interface. Holes at the interface communicate with interface states, and equilibrium is achieved between the SiC valence band and the interface states. This is to say that positive charges are accumulated in the interface states present between the SiC Fermi level and metal Fermi level. The interface-state positive charges induce a shift of the SiC substrate Si $2p$ peak. When a sufficiently high negative bias is applied to SiC, on the other hand, the band bending in SiC greatly decreases and consequently electrons in the bulk transfer to the interface. In this case, an equilibrium is achieved between interface states and SiC conduction band. Under x-ray irradiation, in fact, a current flows in the whole bias region (cf. Fig. 5), showing that one of the SiC bands always equilibrates with interface states. Hence we can conclude that the interface Fermi level always coincides with the SiC bulk Fermi level because of the equilibrium, and thus the energy distribution of the interface-state density can be obtained from the analysis of the bias-induced shift of the substrate Si $2p$ peak.

For the dry-oxide layers, a sharp interface state peak is present at 1.8 eV above the VBM, while such a peak is not present for the wet-oxide layers formed at 1000 °C. We think that the 1.8-eV interface states are induced during the formation of interfacial graphitic carbon, for the following reasons. It is reported that loss of Si occurs during high-temperature heat treatments of SiC, resulting in the formation of graphitic carbon at the SiC surface.[31,32] In the present study, we also observed the formation of interfacial graphitic carbon when POA was performed at 1150 °C, while no formation was observed when the POA temperature was lowered to 950 °C. This result agrees with the recent observation that no carbon species is formed in the case of low-temperature oxidation (500–650 °C) of clean SiC(0001)(3×3) surfaces.[12,13] It is not clear whether, in the presence of the SiO_2 overlayer, this carbon accumulation results from the Si desorption or not, but we think that atoms in the interfacial region become mobile at high temperatures, resulting in the carbon accumulation. Even after POA at 1150 °C, however, the interface-state density is much lower than the concentration of graphitic carbon.[33] Therefore, the following possibilities are considered for the 1.8-eV interface states: (i) Defect states such as carbon vacancies are introduced near the interface during the formation of interfacial graphitic carbon and these defect states possess an energy level at 1.8 eV above the VBM, and (ii) graphitic carbon only with a special structure acts as interface states. In the case of wet oxidation, graphitic carbon is not formed because of the reaction of carbon with water to result in hydrocarbon which desorbs easily. If the 1.8-eV interface states were due to reason (i), the interface states would be still present after the removal of graphitic carbon by the reaction of water. This is not the case, and thus reason (ii) is more probable. The narrow width of the 1.8-eV peak indicates that the environment of the defect states is monotonous. This result also supports the view that graphitic carbon only with a special structure acts as the interface states.

There are two possibilities for the broad structure at ~2 eV above the VBM: (i) dangling bond states and (ii) states arising from the deviation of the bond angles and bond lengths from the bulk values.[34] The states due to reason (ii) are expected to have a U-shaped energy distribution [i.e., the interface-state density decreasing with the energy from the

conduction (or valence) band to the midgap] because the probability of the deviation decreases with its magnitude. The observed interface-state spectra do not possess a U-shaped feature, and moreover the interface-state density is high only above the midgap. These facts exclude possibility (ii), and thus the broad structure is more probably attributable to dangling bond states at the interface.

The large width of the 2-eV peak probably results from the variation in the environments of dangling bond states. It is likely that dangling bonds weakly interact with the nearest Si or oxygen atom in the SiO_2 layer, and the variation in the magnitude of the interaction due to various distances causes the broadening of the 2-eV peak. In the case of interface states present at SiO_2/Si interfaces, theoretical calculations using a density functional theory method show that Si dangling bond energy varies greatly due to the interaction with atoms in the SiO_2 layer.[35]

The density of the 2-eV interface states for the wet-oxide layers is nearly the same as that for the dry-oxide layers, indicating that dangling bond states at the SiC/SiO_2 interface are not eliminated by reaction with H or OH. In the case of SiO_2/Si interfaces, Si dangling bond interface states are effectively passivated by hydrogen due to the formation of Si-H bonds.[36,37] In the case of the formation of SiO_2 from SiC in wet oxygen, high temperatures above 1000 °C—much higher than the temperature at which Si-H bonds are ruptured [550–600 °C (Refs. 38 and 39)]—are required, and therefore Si dangling bond interface states cannot be passivated by hydrogen formed by the decomposition of water.

The lower interface-state density for wet oxidation than that for dry oxidation is often attributed to the passivation of Si dangling bonds by H and OH.[10] It is also reported that the density of interface states at SiO_2/SiC interfaces is decreased by high-temperature heat treatments at around 800 °C in hydrogen[40] or moderate temperature heat treatments (up to 400 °C) in an atomic hydrogen ambient.[41] In these studies, the decrease in the interface-state density was tentatively attributed to the passivation of dangling bonds.[39,40] The present study suggests that the removal of graphitic carbon at the interface by the reaction with hydrogen is an important factor in the decrease of the interface-state density.

For the MOS diodes fabricated in the present study, a current flows through the ultrathin SiO_2 layer. In general, the dark current density $J_{\rm dark}$ is written as

$$J_{\rm dark}=\sum_i P_i J_i^0\left[\exp\left(-\frac{eV}{n_0 n_i kT}\right)-1\right], \tag{10}$$

where P_i and J_i^0 are the transmission probability through the SiO_2 layer and the dark saturation current density, respectively, for the ith current component, V is the bias voltage applied to an n-type semiconductor with respect to the metal electrode, and n_0 and n_i are the n values (ideality factors) which do not and do depend on the kind of the current components.[42] The physical meaning of n_0 is that a part of the external bias voltage V is applied across the oxide layer, $\Delta V_{\rm ox}$, mainly due to the presence of interface states,[43] and consequently the net bias voltage applied to the semiconductor, V_s, is reduced by this magnitude:

$$n_0=\frac{V}{V_s}=\frac{V}{V-\Delta V_{\rm ox}}. \tag{11}$$

Since $\Delta V_{\rm ox}$ is mainly determined by the energy distribution of interface states, as Eq. (7) shows, n_0 depends on the bias voltage. On the other hand, n_i depends on the current flow mechanism, e.g., unity for the majority-carrier thermionic emission current and the minority-carrier diffusion current, and nearly two for the interface-state recombination current.[44]

The dark current density due to majority-carrier thermionic emission, $J_{\rm dark}$, is expressed as[30]

$$\begin{aligned} J_{\rm dark}&=PA^*\exp\left(-\frac{\phi}{kT}\right)\left[\exp\left(-\frac{eV}{n_0 kT}\right)-1\right]\\ &\approx PA^*\exp\left[-\frac{1}{kT}\left(\phi+\frac{eV}{n_0}\right)\right]\\ &=PA^*\exp\left(-\frac{E_{C,b}-E_{F,b}}{kT}\right)\exp\left(-\frac{eV_b}{kT}\right), \end{aligned} \tag{12}$$

where A^* is the modified Richardson constant, ϕ is the barrier height at zero bias, $E_{C,b}$ and $E_{F,b}$ are the energies of the bulk conduction band and bulk Fermi level, respectively, and V_b is the SiC band bending given by

$$eV_b=\phi-(E_{C,b}+E_{F,b})+\frac{eV}{n_0}. \tag{13}$$

The separation between the dark I-V curves for the wet- and dry-oxide layers of ~0.2 V reasonably agrees with the difference in the barrier height ϕ between these oxide layers [which difference is identical to that in the interface Fermi level, i.e., 1.6 and 1.8 eV above the VBM for the wet- and dry-oxide layers, respectively (cf. Fig. 3)], supporting the view that the majority-carrier thermionic emission current is the dominant component of the dark current.

Under x-ray irradiation, electron-hole pairs are generated, followed by their separation by an electrical field in the space-charge layer. The total current density J is given by the sum of the dark current density $J_{\rm dark}$ and the constant photocurrent density $J_{\rm ph}$ (Ref. 30):

$$J=J_{\rm dark}+J_{\rm ph}=PA^*\exp\left[-\frac{1}{kT}\left(\phi+\frac{eV}{n_0}\right)\right]+J_{\rm ph}. \tag{14}$$

Equation (14) shows that for the ideal case (i.e., in the absence of interface states), the I-V curve under irradiation is simply given by the parallel shift of the I-V curve measured in the dark by the magnitude of the photocurrent density. The ideal I-V curves under irradiation are depicted by the dashed lines in Fig. 5. The I-V curve observed for the wet-oxide layers (curve *a*) slightly deviates from the ideal curve (~0.4 V deviation), while that for the dry-oxide layers (curve *b*) greatly deviates from it (~0.8 V deviation) for the following reason: In the case of the dry-oxide layers, high-density interface states are present below the Fermi level (which cor-

responds to the positive-bias region), as shown in Fig. 3(c). In the dark, these interface states cannot capture holes (minority carriers) because of the extremely low hole density due to the wide gap. Under x-ray irradiation, on the other hand, holes are generated and they are transferred to the interface by the electrical field in the SiC space-charge layer. Under a positive bias, the interfacial Fermi level is shifted downward and holes are newly accumulated in the interface states present between the metal Fermi level and SiC Fermi level. These positive charges at the interface states shift the SiC band edge downward, and consequently the band bending in SiC is decreased by the same magnitude, resulting in the shift of the *I*-*V* curve in the positive-bias direction.

For the majority-carrier thermionic emission current, the current density is determined only by the magnitude of the band bending in SiC, V_b, as is evident from Eq. (12). In Fig. 5, points at which the magnitudes of the band bending in SiC with the wet- and dry-oxide layers are the same are denoted by $A-C$, which were determined from XPS measurements under bias. It is clearly seen that the current densities are the same when the magnitudes of the band bending are identical, indicating that the majority-carrier thermionic emission is a dominant current flow mechanism. We can therefore conclude that the *I*-*V* curves under x-ray irradiation are determined by the band bending in SiC, which is in turn determined by the interface-state charges, and that the interface states do not act as effective recombination centers for holes and electrons.

VI. CONCLUSION

Interface-state spectra for the 6*H*-SiC(0001)-based MOS diodes with an ultrathin SiO_2 layer have been obtained from XPS measurements under bias, and the analysis of the results leads to the following conclusions.

(1) Wet-oxide layers formed at 1000 °C have a broad interface-state peak at ~2 eV above the VBM, and this peak is attributed to Si dangling bonds at the interface. The large width of the peak is caused by the interaction of the dangling bonds with a Si or oxygen atom in the SiO_2 layer.

(2) By an increase in the wet-oxidation temperature from 1000 to 1150 °C, a sharp interface-state peak newly appears at 1.8 eV above the VBM. The formation of graphitic carbon at the interface occurs when POA is performed at 1150 °C, while it is not formed by POA at 950 °C. Therefore, the 1.8-eV interface-state peak has been tentatively attributed to graphitic-carbon-related interface states. We think that graphitic carbon only with a special structure acts as the 1.8-eV interface states.

(3) In the case of wet oxidation at high temperatures, graphitic carbon formed at the interface is partially removed by the reaction with H and OH, while such reactions do not occur in the case of the dry oxidation. Therefore, the 1.8-eV interface-state density for the dry-oxide layers is higher than that for the wet-oxide layers.

(4) The density of the Si dangling bond interface states at ~2 eV does not strongly depend on the oxidation temperature and atmosphere, while that of the graphitic-carbon-related interface states at 1.8 eV is greatly dependent on them.

(5) The *I*-*V* curve measured under x-ray irradiation for the dry-oxide layers greatly deviates from the ideal *I*-*V* curve, while the deviation for the wet-oxide layers is much smaller. The interface states affect the *I*-*V* curves under x-ray irradiation by changing the SiC band bending due to the accumulated charges, but the electron-hole recombination at the interface states is negligible.

(6) Majority-carrier thermionic emission is the dominant mechanism of the dark current. The *I*-*V* curve in the dark depends on the SiC Fermi level, which is in turn determined by interface-state charges at zero bias.

*Electronic address: h.kobayashi@sanken.osaka-u.ac.jp
†Present address: Institute of Applied Physics, University of Tsukuba, 1-1-1 Tennodai, Tsukuba, Ibaraki 305-8573, Japan.

[1] R. F. Davis and J. T. Glass, Adv. Solid State Chem. **2**, 1 (1991).
[2] J. W. Palmour, J. A. Edmond, H. S. Kong, and C. H. Carter, Jr., Physica B **185**, 461 (1993).
[3] J. W. Palmour, J. A. Edmond, H. S. Kong, and C. H. Carter, Jr., in *Amorphous and Crystalline Silicon Carbide IV*, edited by C. Y. Yang, M. M. Rahman, and G. L. Harris (Springer, Berlin, 1992), Vol. 71, p. 289.
[4] B. J. Baliga, IEEE Trans. Electron Devices **43**, 1717 (1996).
[5] R. J. Trew, J.-B. Yan, and P. M. Mock, Proc. IEEE **79**, 598 (1991).
[6] J. N. Shenoy, G. L. Chindalore, M. R. Melloch, J. A. Cooper, Jr., J. W. Palmour, and K. G. Irvine, J. Electron. Mater. **24**, 303 (1995).
[7] L. A. Lipkin and J. W. Palmour, J. Electron. Mater. **25**, 909 (1996).
[8] T. Ouisse, N. Bécourt, C. Jaussaud, and F. Templier, J. Appl. Phys. **75**, 604 (1994).
[9] N. N. Singh and A. Rys, J. Electrochem. Soc. **145**, 299 (1998).
[10] S. Zaima, K. Onoda, Y. Koida, and Y. Yasuda, J. Appl. Phys. **68**, 6304 (1990).
[11] H. Yano, T. Kimoto, H. Matsunami, M. Bassler, and G. Pensl, Mater. Sci. Forum **338–342**, 1109 (2000).
[12] F. Amy, P. Soukiassian, Y.-K. Hwu, and C. Brylinski, Appl. Phys. Lett. **75**, 3360 (1999).
[13] F. Amy, P. Soukiassian, Y. K. Hwu, and C. Brylinski, Phys. Rev. B **65**, 165323 (2002).
[14] C. Raynaud, J.-L. Autran, B. Balland, G. Guillot, C. Jaussaud, and T. Billon, J. Appl. Phys. **76**, 993 (1994).
[15] J. A. Cooper, Jr., Phys. Status Solidi A **162**, 305 (1997).
[16] J. Fernández, P. Godignon, S. Berberich, J. Rebollo, G. Brezeanu, and J. Millán, Solid-State Electron. **39**, 1359 (1996).
[17] A. Goetzberger and J. C. Irvin, IEEE Trans. Electron Devices **ED-15**, 1009 (1968).
[18] J. Campi, Y. Shi, Y. Luo, F. Yan, and J. H. Zhao, IEEE Trans. Electron Devices **ED-46**, 511 (1999).
[19] A. Suzuki, H. Ashida, N. Furui, K. Mameno, and H. Matsunami, Jpn. J. Appl. Phys., Part 1 **21**, 579 (1982).
[20] N. Inoue, T. Kimoto, H. Yano, and H. Matsunami, Jpn. J. Appl. Phys., Part 2 **36**, L1430 (1997).
[21] H. Kobayashi, K. Namba, T. Mori, and Y. Nakato, Phys. Rev. B **52**, 5781 (1995).
[22] Y. Yamashita, K. Namba, Y. Nakato, Y. Nishioka, and H. Koba-

yashi, J. Appl. Phys. **79**, 7051 (1996).
[23] H. Kobayashi, A. Asano, S. Asada, T. Kubota, Y. Yamashita, K. Yoneda, and Y. Todokoro, J. Appl. Phys. **83**, 2098 (1998).
[24] Y. Yamashita, A. Asano, Y. Nishioka, and H. Kobayashi, Phys. Rev. B **59**, 15 872 (1999).
[25] T. Sakurai, E. A. de Vasconcelos, T. Katsube, Y. Nishioka, and H. Kobayashi, Appl. Phys. Lett. **86**, 96 (2001).
[26] R. Flitsch and S. I. Raider, J. Vac. Sci. Technol. **12**, 305 (1975).
[27] H. Kobayashi, K. Namba, Y. Yamashita, Y. Nakato, T. Komeda, and Y. Nishioka, J. Appl. Phys. **80**, 1578 (1996).
[28] B. Hornetz, H-J. Michel, and J. Halbritter, J. Mater. Res. **9**, 3088 (1994).
[29] W. K. Choi, T. Y. Ong, L. S. Tan, F. C. Loh, and K. L. Tan, J. Appl. Phys. **83**, 4968 (1998).
[30] S. M. Sze, *Physics of Semiconductor Devices*, 2nd ed. (Wiley, New York, 1981), Chap. 14.
[31] S. Adachi, M. Mohri, and T. Yamashina, Surf. Sci. **161**, 479 (1985).
[32] L. I. Johansson, F. Owman, and P. Mårtensson, Phys. Rev. B **53**, 13 793 (1996).
[33] H. Kobayashi, T. Sakurai, M. Nishiyama, and Y. Nishioka, Appl. Phys. Lett. **78**, 2336 (2001).
[34] R. B. Laughlin, J. D. Joannopoulos, and D. J. Chadi, in *The Physics of* SiO_2 *and Its Interfaces*, edited by S. T. Pantelides (Pergamon, New York, 1978), Chap. 6.
[35] T. Kubota, A. Asano, Y. Nishioka, and H. Kobayashi, J. Chem. Phys. **111**, 8136 (1999).
[36] M. L. Reed and J. D. Plummer, J. Appl. Phys. **63**, 5776 (1988).
[37] T. W. Hickmott, J. Appl. Phys. **48**, 723 (1977).
[38] P. J. Caplan, E. H. Poindexter, B. E. Deal, and R. R. Razouk, J. Appl. Phys. **50**, 5847 (1979).
[39] F. B. McLean, IEEE Trans. Nucl. Sci. **NS-27**, 1651 (1980).
[40] K. Fukuda, S. Suzuki, T. Tanaka, and K. Arai, Appl. Phys. Lett. **76**, 1585 (2000).
[41] V. Raineri, S. Lombardo, P. Musumeci, A. M. Maktari, and L. Calcagno, Mater. Sci. Forum **353–356**, 639 (2001).
[42] H. Kobayashi, T. Ishida, Y. Nakato, and H. Tsubomura, J. Appl. Phys. **69**, 1736 (1991).
[43] H. C. Card and E. H. Rhoderick, J. Phys. D **4**, 1589 (1971).
[44] M. Y. Ghannam and R. P. Mertens, IEEE Trans. Electron Devices **ED-10**, 242 (1989).